

Poly(acrylic acid/acrylamide/sodium humate) Superabsorbent Hydrogels for Metal Ion/Dye Adsorption: Effect of Sodium Humate Concentration

Tripti Singh, Reena Singhal

Department of Plastic Technology, Harcourt Butler Technological Institute, Kanpur, Uttar Pradesh 208002, India

Received 20 May 2011; accepted 3 August 2011

DOI 10.1002/app.35435

Published online 7 January 2012 in Wiley Online Library (wileyonlinelibrary.com).

ABSTRACT: A series of novel superabsorbent hydrogels based on acrylic acid (AAc), acrylamide (AM), and sodium humate (SH) were prepared by free-radical solution copolymerization for removal of dye and metal ion from waste water. Ammonium per sulfate was used as initiator and *N,N'* methylene bisacrylamide as crosslinker. The hydrogels were characterized with the help of FTIR and SEM. In this study the concentration of SH was varied in the range of 0.50–4.76 wt % based on total monomer content and the resulting hydrogels were investigated for the effect of SH on swelling and diffusion kinetic parameters such as equilibrium swelling ratio, initial swelling rate, swelling rate constant, maximum swelling at equilibrium, and type of diffusion, etc. Hydrogel having 2.43 wt % SH content showed the maximum water absorbency of 724 g of water per gram of hydrogel. Swelling exponent found in the range 0.68–0.79 thus suggesting Non-Fickian diffu-

sion mechanism. The swelling behavior was also studied in different concentrations of salt solutions [sodium chloride (NaCl), magnesium chloride (MgCl₂), and ferric chloride (FeCl₃)]. The synthesized superabsorbent hydrogels were used for the adsorption of Cu²⁺ ions and methylene blue (MB) dye from their aqueous solutions. The influence of SH concentration on the Cu²⁺ ions and MB molecules binding capacity of hydrogels was tested. The chelation behavior was modeled using Langmuir isotherm. The maximum binding capacity for Cu²⁺ ion was 299 mg/L at 1000 mg/L, initial Cu²⁺ ion concentration and 269 mg/L at 320 mg/L, initial MB dye molecules concentration per gm of AAc/AM/SH containing 2.43 wt % SH content. © 2012 Wiley Periodicals, Inc. *J Appl Polym Sci* 125: 1267–1283, 2012

Key words: hydrogels; sodium humate; acrylamide; acrylic acid; swelling behavior; heavy metal ion; dye; diffusion

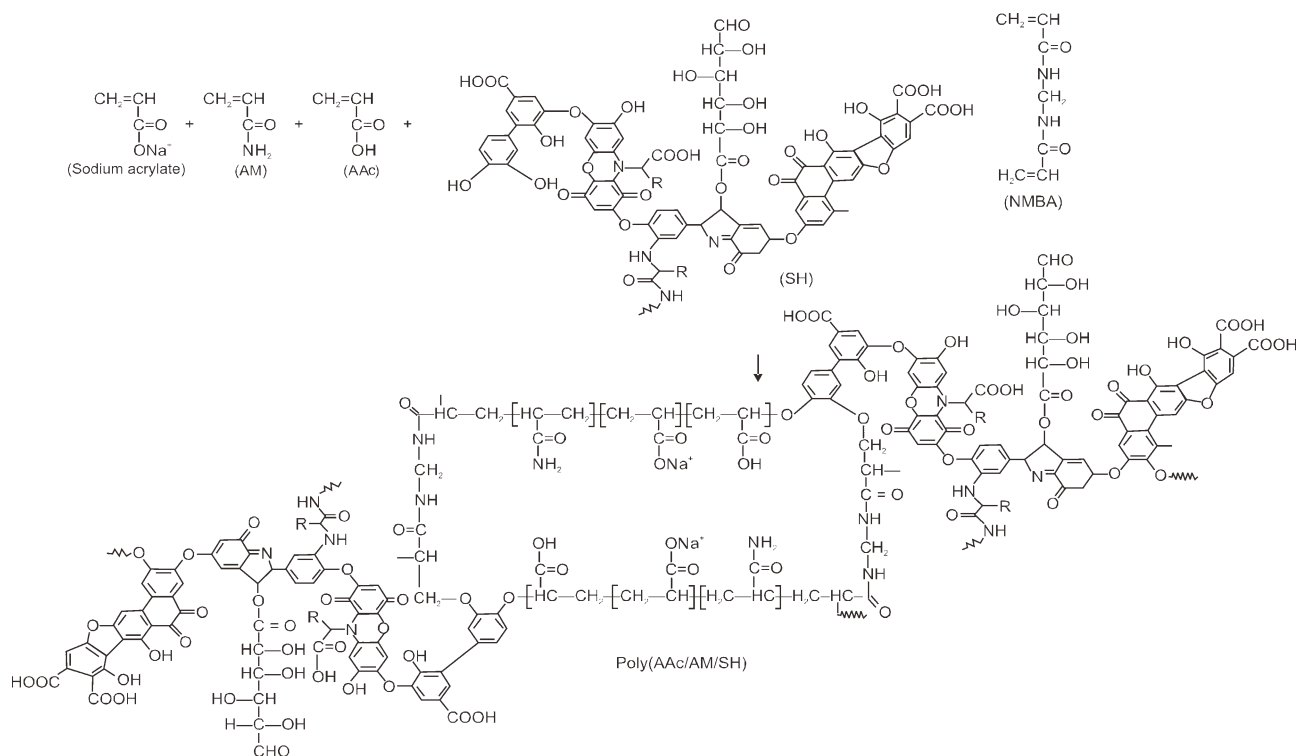
INTRODUCTION

Hydrogels are chemically or physically crosslinked hydrophilic polymers, which can absorb large amounts of water, saline, or physiological solutions without dissolving and losing their shapes. Superabsorbent hydrogel is a special class of hydrogels having very high swelling capacities. They are moderately crosslinked three-dimensional hydrophilic network polymers that can absorb and retain considerable amounts of aqueous fluids even under pressure. Because of their excellent properties such as hydrophilicity, high swelling capacity, and biocompatibility, superabsorbent hydrogels have found potential application in many fields such as agriculture,¹ horticulture,² hygiene products,³ drilling fluid additives,⁴ sealing material,⁵ polymer concrete suited for use in repairing cracks,⁶ dew preventing coating,⁷ fire fighting,⁸ and drug delivery.⁹ Superabsorbent hydrogels were also developed for the adsorp-

tion of some cationic dyes, heavy metal ions, and sebum albumin.^{10–12}

In the last decade, a tremendous increase in the use of heavy metal ions and dyes contaminant volume has posed many serious environmental problems because of their toxicity to many life forms.¹³ They are classified as stable and persistent environmental toxic substances because they cannot be degraded and destroyed by chemical or biological remediation processes.¹⁴ Numerous research efforts are being done to develop methods of treatment for waste water. These methods are chemical precipitation, filtration, chelating ion exchange, electrochemical treatment, reverse osmosis, neutralization, and adsorption.¹⁵ Among these techniques, adsorption process is generally recommended for the removal of heavy metal ions and dyes because of its easy handling, high efficiency, regenerability, availability of different adsorbents, and cost effectiveness.¹⁶ In recent years, it was determined that hydrogels having functional groups such as, carboxylic acid, amine hydroxyl, and sulfonic acid groups can be used as complex agent for the removal of metal ions from aqueous solutions¹⁷; therefore, the synthesis of superabsorbent hydrogels with chelating groups have received considerable attention for rapid and inexpensive metal ion/dye separation and concentration.

Correspondence to: R. Singhal (reena_singhal123@rediffmail.com or reenasinghal123@gmail.com).



Scheme 1 Synthesis of superabsorbent hydrogels poly (AAc/AM/SH).

The first step in the preparation of the hydrogels is the selection of a highly hydrophilic or even water soluble polymer.¹⁸ The majority of the important superabsorbents are now a day manufactured from synthetic hydrophilic polymers such as poly(acrylic acid), partially neutralized poly(acrylic acid), and their copolymer hydrogels of poly(acrylamide). This is due to their higher water absorption and retention capacity for longer time, which is an essential criterion to various applications. The synthetic polyacrylates derived from acrylic acid (AAc) have emerged as an important absorbent because of its superior price to efficiency balance i.e., AAc is cheap and easy to polymerize to products of high molecular weight. Another benefit is that it has carboxylic group leading to application in metal ion/cationic dye removal, as the gels containing acid groups have been used to bind ions including some heavy metals¹⁷ from aqueous media. Polyacrylamide and copolymers of polyacrylamide have the capability to absorb water and capable of metal ion/dye adsorption as it provide acidic group after hydrolysis.

Humic acid is a natural product and it is a principal component of humic substances. It is composed of multifunctional aliphatic components and aromatic constituents and contains large number of functional hydrophilic groups (such as carboxylates and phenolic hydroxyls).¹⁹ It is a complex mixture of many different acids containing carboxyl and phenolate groups so that the mixture behaves functionally as a dibasic acid or occasionally as a tribasic

acid. Sodium humate (SH) form complexes/chelates with cationic dye/metal ions due to the presence of these carboxylate and phenolate groups. The chemical structure of monomers and crosslinked polymer is shown in Scheme 1. It was reported that presence of humic acid/humates can benefit the adsorption of heavy metal ions and dyes. Yi et al.²⁰ synthesized SH/poly(*N*-isopropylacrylamide) by solution polymerization and examined swelling and decoloring properties of SH/PNIPA hydrogels. Humic substances could be adsorbed on the mineral particles by which they would promote the adsorption of some heavy metal ions/dye.

Li et al.²¹ prepared polyacrylamide-polyacrylic acid hydrogel and investigated its binding properties for various metal ions under varying conditions of ionic strength, metal concentration, pH, and time. Liu et al.²² synthesized chitosan-g-poly(acrylic acid)/SH by graft polymerization in aqueous solution and find out that water absorbency enhanced from 135 to 183 gram of water absorbed by per gram of hydrogel (gg^{-1}) by introducing 10 wt % SH and afterwards it decreased. Hua and Wang²³ prepared sodiumalginate-g-poly(acrylic acid)/SH superabsorbent by graft copolymerization, and studied the effects of crosslinker, sodium alginate, and SH content on water absorbency of the superabsorbent.

This article reports the synthesis of a series of multifunctional superabsorbent hydrogel composed of acrylic acid-acrylamide and SH with varying SH concentration by solution polymerization using *N,N*-methylene bisacrylamide (NMBA) as crosslinker and

TABLE I
Various Feed Ratios of AAc, AM, and SH for
Synthesizing a Series of Poly (AAc\AM\SH)
Superabsorbent Hydrogels

Sample designation	Monomer ratio (weight ratio) (AAc/AM/SH)	Monomer ratio wt % (AAc/AM/SH)	Weight of SH (gm)
S ₀	1/1/0	50/50/00	0.00
S ₁	1/1/0.01	49.75/49.75/0.50	0.07
S ₂	1/1/0.02	49.5/49.5/0.99	0.14
S ₃	1/1/0.03	49.26/49.26/1.47	0.21
S ₄	1/1/0.04	49.01/49.01/1.96	0.28
S ₅	1/1/0.05	48.78/49.78/2.43	0.35
S ₆	1/1/0.06	48.54/48.54/2.91	0.42
S ₇	1/1/0.07	48.30/48.30/3.38	0.48
S ₈	1/1/0.08	48.07/48.07/3.84	0.54
S ₉	1/1/0.09	47.84/47.84/4.30	0.63
S ₁₀	1/1/0.10	47.61/47.61/4.76	0.70

Other conditions: AAc, 7 gm; AM, 7 gm; APS, 0.40 wt %; NMBA, 0.20 wt %; molar ratio of AM to AAc, 1.01 mol mol⁻¹; distilled water, 30 mL; temperature 50°C.

Ammonium per sulfate (APS) as initiator. The effect of SH content variation on swelling and diffusion characteristics, and its effect on Cu²⁺ ion/MB molecules removal was investigated. The parameters influencing the adsorption capacity of the hydrogel for example effect of SH content, initial Cu²⁺ ions, and methylene blue dye concentration were also investigated. The synthesized hydrogels were characterized by FTIR and SEM analysis.

EXPERIMENTAL

Materials

Acrylic acid [(AAc), analytical grade], acrylamide [(AM), analytical grade], ammonium per sulfate [(APS), analytical grade], sodium hydroxide [(NaOH), analytical grade], magnesium chloride [(MgCl₂), analytical grade], ferric chloride [(FeCl₃), analytical grade], copper sulfate [(CuSO₄), analytical grade], and *N,N*-methylene bisacrylamide [(NMBA), analytical grade], were purchased from CDH New Delhi, India. Methylene blue dye (spectroscopic grade, Qualigens Fine Chemicals, Mumbai, India) was used as received. Methanol (analytical grade) was purchased from Qualikems, New Delhi. AM was recrystallized from methanol before use. Sodium humate [(SH), analytical grade], (supplied from Aldrich) was used as received. Double distilled water was used throughout the experiments.

Synthesis of poly (AAc-co-AM-co-SH) hydrogels

A series of superabsorbent poly (AAc-co-AM-co-SH) hydrogels having initiator (APS) 0.40 wt % of total

monomer, crosslinker (NMBA) concentration 0.20 wt % of total monomer were synthesized. Molar ratio of AM to AAc was 1.01 mol mol⁻¹ for all the (AA/AM/SH) hydrogel. The actual feed compositions are shown in Table I

Polymerization procedure of poly (AAc-co-AM-co-SH) hydrogels

Depending upon AAc, AM, and SH monomer based hydrogels with different amount of SH were synthesized as follows. AAc and AM were dissolved in 30 mL distilled water. Then the NaOH solution was added to neutralize the above solution and its pH was determined with the help of pH meter. NaOH solution was added drop by drop till the mixture shows pH = 4. After that reaction mixture was introduced in a 250 mL three-neck flask equipped with a stirrer, a reflux condenser, and a nitrogen inlet. NMBA was added to the monomer solution and then appropriate amount of SH was dispersed into mixed solution. After being purged with nitrogen for 30 min to remove the oxygen dissolved in the solution, the mixed solution was heated in a thermostat oil bath at 50°C, gradually and then the initiator, APS, was introduced into the flask. The solution was stirred vigorously and a nitrogen atmosphere was maintained until the gel was formed. After polymerization the reaction product was removed and cut into small pieces (0.1–0.5 cm in thickness) and washed with methanol and water, and then dried in an oven at 60°C until the weight of the product was constant.

Dynamic and equilibrium swelling studies

The completely dried preweighed hydrogel sample was placed in 1000 mL distilled water (sink condition) at room temperature 30.0 ± 5.0°C. The swollen gel was taken out at regular time intervals and its surface was quickly blotted free of water by using filter paper. It was then weighed and placed in the same bath. The mass measurements were continued till the attainment of the equilibrium.

The equilibrium swelling ratio (S_{eq}) was determined following the conventional gravimetric method using the following equation:

$$S_{eq}(\text{g/g}) = \frac{\text{Equilibrium swollen weight} - \text{dry weight}}{\text{dry weight}} \quad (1)$$

To examine the controlling mechanism of the swelling process, several kinetic models are used to test experimental data. The overall kinetics of a hydrogel involving long swelling periods may be described with Schotts second-order kinetics,²⁴

TABLE II
Swelling Kinetic Parameters [Based on eq. (3)], Diffusion Exponent (n), Diffusion Constant (k), Diffusion Coefficient (D), and Water Sorption Rate Constant (k_w) of AAC/AM/SH Superabsorbent Hydrogel Systems

Sample designation	Initial swelling rate r_i $g_{\text{water}}/g_{\text{gel}}$ min	Swelling rate constant k_s ($\times 10^6$) $g_{\text{gel}}/g_{\text{water}}$ min	Theoretical equilibrium swelling $g_{\text{water}}/g_{\text{gel}}$	Swelling exponent (n)	Gel characteristic constant k ($\times 10^6$)	Diffusion coefficient D ($\times 10^3$) cm^2m^{-1}	Water sorption rate constant k_w ($\times 10^3$)
S ₁	3.55	14.31	498	0.68	91.2	49.69	4.50
S ₂	3.65	11.86	555	0.69	72.6	50.00	4.40
S ₅	4.45	7.52	769	0.70	54.9	51.30	3.90
S ₇	1.14	5.90	439	0.77	9.14	36.43	2.30
S ₁₀	1.08	6.80	400	0.79	5.79	35.15	2.20

$$\frac{dS}{dt} = k_s(S_{\text{eq}} - S)^2 \quad (2)$$

where k_s is rate constant of swelling and S_{eq} (or $S_{\text{eq}}\%$) denotes the swelling percent at equilibrium. After definite integration by applying the initial condition $S_{\text{eq}} = S_0$ at time $t = t_0$ and $S_{\text{eq}} = S$ at time $t = t$ then eq. (2) becomes

$$\frac{t}{S} = A + Bt \quad (3)$$

Where A and B are two coefficients whose physical significance is interpreted as follows; at a long range time $Bt \gg A$ and according to eq. (3) $B = \frac{1}{S_{\text{eq}}}$, i.e., it is the reciprocal of the equilibrium water uptake. On the contrary, at a very short range time $A \gg Bt$ and in the limit equation becomes,

$$\lim_{t \rightarrow 0} \left(\frac{dS}{dt} \right) = \frac{1}{A} \quad (4)$$

Therefore the intercept A is the reciprocal of the initial swelling rate r_i or $\frac{1}{k_s S_{\text{eq}}^2}$. To test the kinetic model, t/S vs. t graphs are plotted and the calculated kinetic parameters are tabulated in Table II.

Analysis of mechanism of water uptake and diffusion coefficient

When a polymer is brought into contact with a solvent, the solvent diffuses into the polymer matrix, thus causing it to swell. This diffusion process involves migration of solvent into preexisting or dynamically formed spaces between macromolecular chains. Swelling of hydrogel involves larger scale segmental motion ultimately resulting into an increased distance of separation between macromolecular chains.²⁵ The portion of the water absorption curve with a fractional water uptake $F(M_t/M_\infty)$ less than 0.60 [as given in Fig. (5)] was analyzed using the following eq. (5),

$$F = kt^n \quad (5)$$

where M_t the mass of water is absorbed at time t and M_∞ is the mass of water absorbed at equilibrium, k is

a characteristic constant of the hydrogel, and the exponential n is a number used to determine the type of diffusion. For $n = 0.45$ – 0.50 , the swelling process is diffusion controlled and was termed Fickian type transport. When $0.50 < n < 1.0$, it indicates non-Fickian or anomalous transport; and $n = 1$ implies Case II (relaxation controlled) transport. The constant n and k were calculated from the slopes and intercepts of the plots of $\ln F$ vs. $\ln t$ from the experimental data and have been summarized in Table II.

The short time approximation method is used for the calculation of diffusion coefficient of AAC/AM/SH hydrogel.²⁶ The short time approximation method is valid for the first 60% of initial swelling. The diffusion coefficients of AAC/AM/SH are calculated from the following relation²⁷

$$F = 4 \left(\frac{Dt}{\pi r^2} \right)^{\frac{1}{2}} - \pi \left(\frac{Dt}{\pi r^2} \right) - \frac{\pi}{3} \left(\frac{Dt}{\pi r^2} \right)^{\frac{3}{2}} \quad (6)$$

where D is in cm^2/min , t in min, and r is the radius of a cylindrical polymer sample. A graphical comparison of eqs. (5) and (6) shows the semi empirical eq. (7),

$$k = 4 \left(\frac{D}{\pi r^2} \right)^{\frac{1}{2}} \quad (7)$$

For hydrogels F vs. $t^{1/2}$ plots are constructed. The diffusion coefficients were calculated from the slopes of the lines and given in Table II.

Water sorption rate

Other important diffusion parameter is water sorption rate constant k_w . According to the water sorption equation^{27,28},

$$-\ln \left(1 - \frac{M_t}{M_\infty} \right) = k_w t + \varepsilon \quad (8)$$

where t is sorption time, k_w is water sorption rate constant at time t , M_∞ is an equilibrium sorption

amount, and ε is a constant. The plots of $-\ln[1 - F]$ vs. t , where $F = \frac{M_t}{M_\infty}$ are constructed. The value of k_w and ε were calculated from the slopes and intercepts, respectively and listed in Table II.

Fourier transforms infrared spectroscopy (FTIR) studies

The FTIR spectra of poly (AAc\AM\SH) superabsorbent were recorded with Perkin Elmer Spectrophotometer using solid pellet potassium bromide (KBr) after completely drying the sample at 60°C upto constant weight.

Scanning electron microscopy

The surface morphology of various poly(AAc\AM\SH) hydrogels was examined under scanning electron microscope (SEM). Dried hydrogels were coated with a thin layer of pure gold in S150 Sputter Coater, and imaged in a SEM (LEO Electron Microscopy, England).

Measurement of Cu²⁺ ions and MB dye molecules adsorption

For the adsorption studies batch experiments were carried out. For this 50 mg of dry hydrogel was introduced in 100 mL of Cu²⁺ ions salt solution and methylene blue dye solution and was left in solution for 48 h, then the gel was taken out and the quantity

of ions/dye left in solution was monitored by UV-VIS spectroscopy.

The calculation of adsorption capacity was performed by the equation

$$q_e = \frac{C_o - C_e}{m} \times V \quad (9)$$

where C_o is the initial concentration of Cu²⁺ ions/MB dye molecules, C_e is the equilibrium concentration; V is the volume of the Cu²⁺ ions/MB dye solution; and m is the mass of hydrogel sample.

Recovery and reusability

Recovery of the Cu²⁺ ions from the superabsorbent hydrogel was carried out in 25 mL of 0.1M HNO₃ solution (elution medium) for 24 h. The hydrogel adsorbed Cu²⁺ ions were placed in the elution medium and stirred with a magnetic stirrer at room temperature. The final Cu²⁺ ions concentration in the aqueous phase was determined by UV-VIS spectroscopy. The elution ratio was calculated from the amount of Cu²⁺ ions adsorbed on the polymer surface and final Cu²⁺ ions concentration in the elution medium. The MB dye molecules were recovered in distilled water. MB adsorbed hydrogel was put in 500 mL distilled water as elution medium and MB desorbed was measured with the help of UV-VIS spectroscopy. Elution ratio was calculated using the following expression-

$$\text{Desorption ratio} = \frac{\text{Amount of Cu}^{2+}\text{ion/MB dye desorbed to the elution medium}}{\text{Amount of Cu}^{2+}\text{ion/MB dye adsorbed on the superabsorbent hydrogel}} \times 100 \quad (10)$$

To determine the reusability of the superabsorbent hydrogels consecutive adsorption desorption cycle was repeated for five times with the same sample.

RESULTS AND DISCUSSION

FTIR spectra

The characterization of pure SH, PAM, PAAc/AM, and PAAc/AM/SH superabsorbent (S₅, S₁₀) was conducted by FTIR technique and shown in [Fig. 1(a-e)], respectively. Comparing with the IR spectrum of PAM [Fig. 1(b)] the absorption band at 1645 cm⁻¹ for the C=O group of the AM and 1029 cm⁻¹ for the C-N stretching of AM shifts to 1670 and 1068 cm⁻¹, respectively in the IR spectrum of PAAc/AM Figure 1(c), suggesting the polymerization reaction of AAc and AM. On comparing with the IR spectrum of pure SH [Fig. 1(a)] the absorption band at 3210 and 3081 cm⁻¹ for N-H stretching and 2360 cm⁻¹ for O-H stretching of carboxylic group,

1708 cm⁻¹ of C=O stretching of carboxylic group and 1600 cm⁻¹ for asymmetrical stretching of COO⁻ are absent in the spectrum of AAc/AM/SH. In addition, the band of SH at 1238 cm⁻¹ (phenolic C-O stretching) has almost disappeared in the spectrum of S₅ [Fig. 1(d)], indicating involvement of carbonyl group and aromatic hydroxyl group of SH in interaction with the N-H group and carbonyl group of AAc and AM. On comparing with the spectrum of S₀ it was found that the peak at 1670 cm⁻¹ attributed to the C=O in AM changes to 1652 cm⁻¹ after the reaction. Similarly, the peaks at 1730 cm⁻¹ (C=O group of carboxyl group), 1570 cm⁻¹ (symmetric stretching of the carboxylate) and 1380 cm⁻¹ (asymmetric stretching of the carboxylate) change to 1715, 1560, and 1400 cm⁻¹, respectively in the spectrum of S₅ superabsorbent hydrogel. In addition, newly appeared asymmetric vibration of C-H bond at 2935 cm⁻¹ indicate that SH is polymerized and crosslinked by the breaking of C=C bond, as well as the new absorption band at 1706 and 1278 cm⁻¹

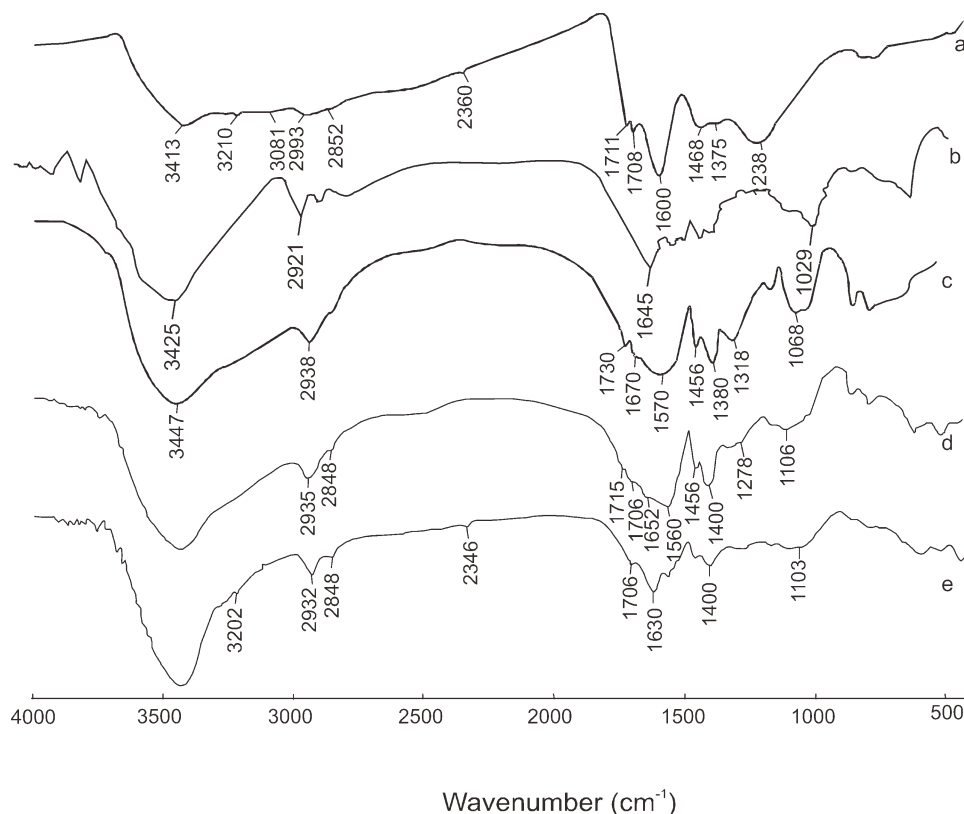


Figure 1 FTIR spectra of (a) SH, (b) PAM, (c) PAAC/AM, (d) PAAC/AM/SH superabsorbent (S_5), and (e) PAAC/AM/SH superabsorbent (S_{10}).

which are attributed to C=O stretching of carboxylic group of SH and aromatic ether is observed, respectively. It indicates that the reaction among AAC, AM, and SH takes place during the copolymerization and they may be connected with the new bond C=O=C in aromatic ether group. In case of spectrum of S_{10} [Fig. 1(e)] the reappearance of the absorption band at 3202 cm^{-1} (N—H stretching), 2346 cm^{-1} (O—H stretching of carboxylic group), and 1706 cm^{-1} (C=O stretching of carboxylic group) shows that at higher concentration SH exists in pure form and acts as only filler.²⁹

Morphological studies

SEM is the most widely employed technique to investigate the shape, size, morphology, crosslink density, and porosity of hydrogels. In the present study, we used this technique to identify the change of surface morphology of superabsorbent hydrogels resulting from the incorporation of SH. The SEM micrograph of superabsorbent hydrogels S_0 , S_1 , S_5 , and S_{10} were observed and shown in Figure 2(a–d). As can be seen from Figure 2(a) hydrogel S_0 showed a dense, and smooth surface with regular ribbed pattern; however, the samples introduced with SH exhibited an undulant, comparatively loose, porous, and coarse surface [Fig. 2(b,c)]. The surface rough-

ness increased with increasing the content of SH and pores and gaps can be observed on the surface of superabsorbent hydrogels S_1 and S_5 when compared with S_0 and S_{10} . In case of hydrogel S_5 [Fig. 2(c)] size of cracks-like structure increased, which provides more space for water penetration that leads to a drastic increase in swelling. Buchholz³⁰ described that the open pores in superabsorbent hydrogels are small reservoirs for water storage, when there is a means to transport the water into open pores. This observation revealed that the incorporation of SH facilitates porosity in the network structure and increases the surface area, which allows enhancement of diffusion of aqueous fluid into the polymeric network resulting in increased water absorbency. Details of the texture shown in case of S_{10} [Fig. 2(d)] shows some coarse irregularly shaped pores and lesser cracks with the dispersed second phase, which showed that excess SH particles do not involve in the formation of polymer network and remain as filler.

Effect of sodium humate concentration on water absorbency

For comparing the performance of hydrogels containing SH, a plain hydrogel S_0 , containing only AAC and AM was synthesized as control. The relationship between equilibrium swelling and SH

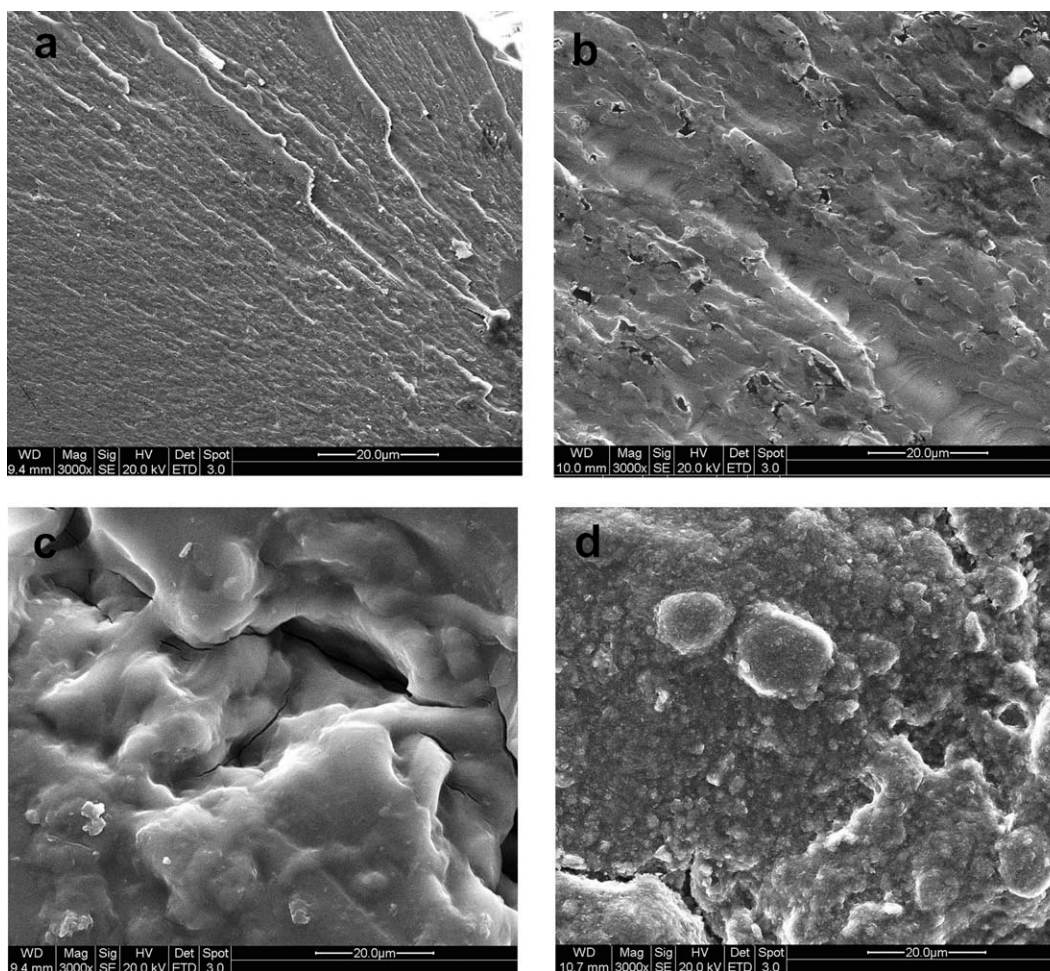


Figure 2 (a) SEM of Poly (AAc/AM/SH) superabsorbent hydrogel S_0 (b) SEM of Poly (AAc/AM/SH) superabsorbent hydrogel S_1 (c) SEM of Poly (AAc/AM/SH) superabsorbent hydrogel S_5 (d) SEM of Poly (AAc/AM/SH) superabsorbent hydrogel S_{10} .

concentration variation is shown in Figure 3. It was observed from the Figure 3 that initially there was moderate increase in equilibrium swelling from 480 to 523 gg^{-1} for the superabsorbent hydrogels S_1 – S_3 having SH concentration 0.50–1.47 wt %. After that the equilibrium swelling ratio shows drastic increase from 523 to 724 gg^{-1} for S_3 to S_5 superabsorbent hydrogels, which have 1.47–2.43 wt % SH concentration in the feed. On further increasing the SH concentration from 2.43 to 4.76 wt % the water absorbency decreased sharply for S_5 – S_{10} hydrogels. The superabsorbent S_5 shows maximum water absorbency of 724 gg^{-1} . The increment in equilibrium swelling values is due to SH is a complex organic macromolecule, contains free and bound phenolic –OH groups, quinine structure, nitrogen and oxygen as bridge unit, –COOH, and –NH₂ groups variously placed on aromatic ring.^{31,32} The species and number of hydrophilic groups in the AAc\AM\SH network were much more, and these functional groups of SH can react with AAc and AM during polymerization process. At the same crosslinker content, the introduction of irregular SH into AAc-AM

polymeric network could decrease the effective cross-linking density, which result in the increasing water absorbency with increasing SH content. However,

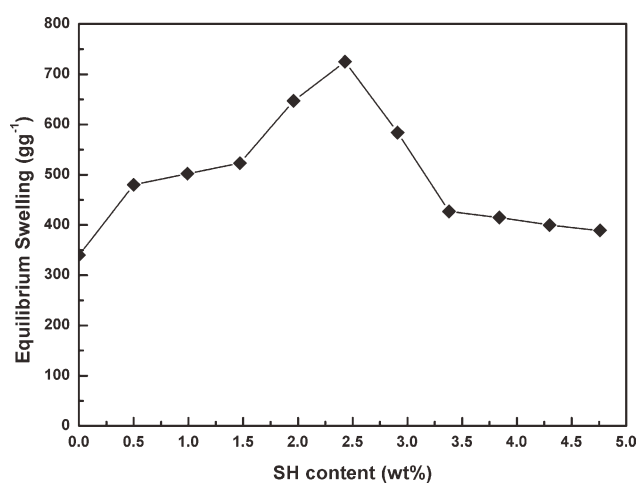


Figure 3 Effect of SH concentration (wt %) on the equilibrium swelling ratio of the synthesized poly (AAc-AM-SH) superabsorbent at 0.40 wt % APS, 0.20 wt % NMBA, molar ratio of AM to AAc 1.01 mol mol⁻¹.

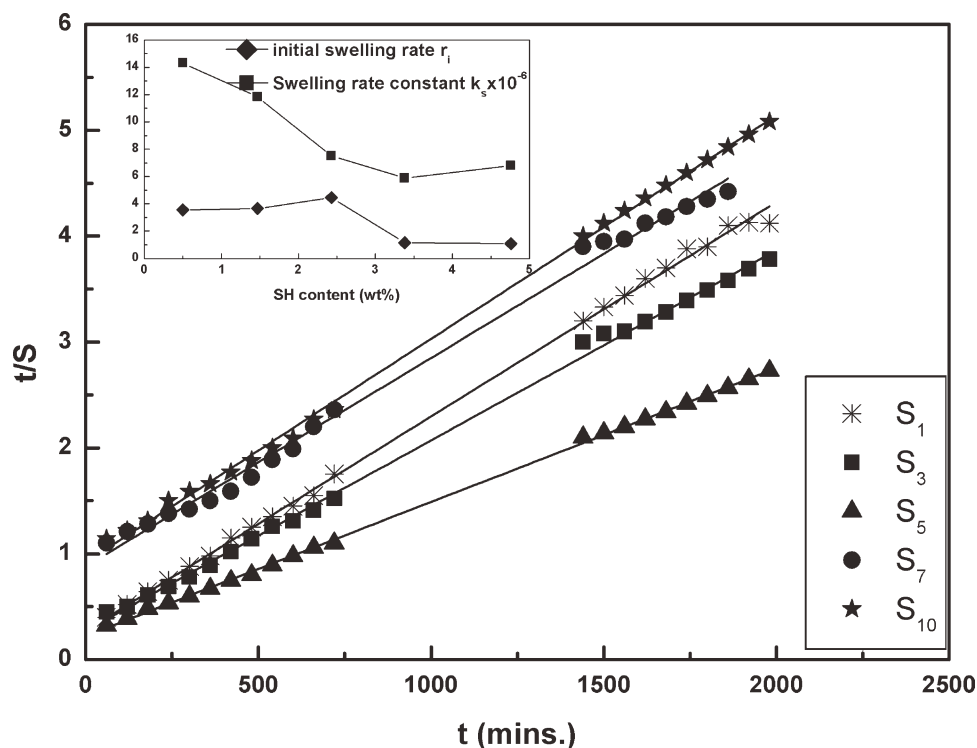


Figure 4 Swelling kinetics curves of AAc-AM-SH superabsorbent at 0.40 wt % APS, 0.20 wt % NMBA, molar ratio of AM to AAc 1.01 mol/mol.

when the SH content increases above 2.43 wt %, the apparent decrease of water absorbency may be attributed to the fact that excessive SH only act as a filler and the amount of hydrophilic groups on the polymeric backbone decreased with the increase of SH content.²³ So it was difficult to form the efficient absorbent three-dimensional structures and the solubility of polymer increased as well as caused the decrease of osmotic pressure difference between the polymeric network and the external solution. It was also reported by Wang and Wang³³ in the case of semi IPN superabsorbent hydrogels based on sodium alginate-*g*-poly(sodium acrylate) and poly(vinyl pyrrolidone) system that the excess of PVP may tangle with the graft polymer chains and the physical crosslinking was formed when the PVP content exceeding 15 wt %. Similar type of result has been observed by Liu et al.²² for superabsorbent hydrogel based on chitosan-*g*-poly(acrylic acid)/SH containing different amount of SH. They found that water absorbency increases from 0 to 10% SH concentration and then decreases and 10 wt % shows the maximum water absorbency at 183 gg^{-1} .

Dynamic swelling studies

Kinetic model is in good agreement with the swelling experiments; the theoretical swelling follows the same trend as the practical one. From the Table II it was identified that there is a significant variation in

their initial swelling rate, theoretical equilibrium swelling, and swelling rate constant because of variation in the SH concentration.

Swelling rate of a superabsorbent hydrogel is significantly influenced by various factors such as size distribution, specific surface area, swelling capacity, and apparent density of polymer.³⁴ It is examined from Figure 4 and Table II that swelling rate increases till the absorbency increases and then it goes down. The initial swelling progress is primarily because of the water penetration into polymeric network through capillary and diffusion.³⁵ Introduction of SH increases the surface area [Fig. 2(b,c)], which results in easy diffusion of solvent molecules into the network, and thus enhance in swelling rate. The results from the Table II show that superabsorbent hydrogel prepared with greater amounts of SH exhibited the lower swelling rate. The percentage of hydrophilic groups (such as $-\text{COOH}$ and $-\text{COO}^-$) on polymeric network for AAc\AM\SH superabsorbent decreased with increasing SH content after a certain level, so the diffusion rate of water penetrating into the superabsorbent decreases. These results indicates that the incorporation of moderate amount of SH is favorable to enhance the swelling rate, but the excessive addition of SH reduced it.

It is clear from the data given in Table II that swelling rate constant decrease with increasing SH concentration. This can be explained based on chelating and hydrophilic nature of SH. As SH concentration

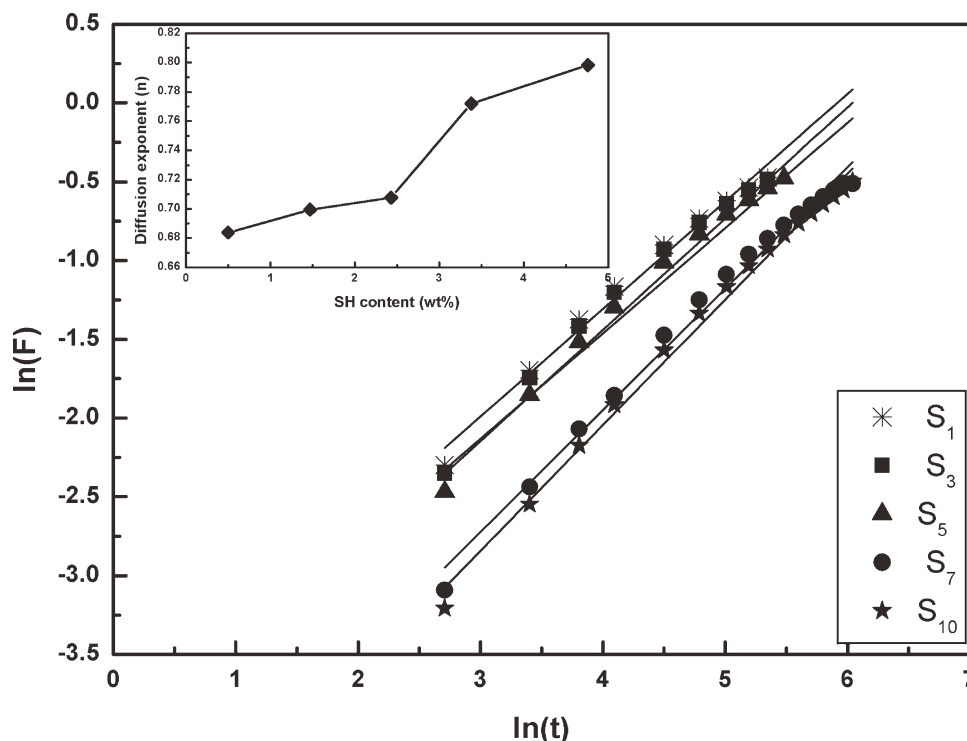


Figure 5 Plots of $\ln(F)$ vs. $\ln(t)$ of AAc-AM-SH superabsorbent at 0.40 wt % APS, 0.20 wt % NMBA, molar ratio of AM to AAc 1.01 mol/mol⁻¹.

increases the capacity of the AAc\AM\SH network to hold water increases. Similar results were found in the study of the swelling behavior of semi-IPNs of starch and poly(acrylamide-*co*-sodium methacrylate).³⁶

Mechanism of water uptake

Table II and Figure 5 clarifies that the swelling exponent n for the samples with varying SH concentrations lie between 0.68 and 0.79; thus suggesting the anomalous or non-Fickian type diffusion.³⁷ It is explained as a consequence of the slow relaxation rate of the polymer matrix, or rates of solvent diffusion and polymer relaxation are comparable.³⁸ As solvent diffuses into the hydrogel, rearrangement of chains does not occur immediately.

The diffusion coefficient, D determined using eq. (6) and is used to study water movement into the hydrogels are shown in Table II. It can be seen that the diffusion coefficient ranges from 35.15×10^{-3} to 51.30×10^{-3} cm² min⁻¹. In this case the relatively higher diffusion coefficients are obtained which is an indication of faster penetration of solvent molecules into the hydrogel. Here the penetration of solvent into hydrogel is easier and the diffusion rate is fast, because there is a hydrophilic interaction between the hydrogel and water.

The results presented in the Table II show that water sorption rate constant changed in the range

2.20×10^{-3} to 4.50×10^{-3} . The reason for this may be hydrophilic characteristics of SH, due to which it interact with the water molecules.

Effect of salts solution on swelling behavior

The characteristic of swelling medium such as salinity has a well known influence on swelling properties of a superabsorbent hydrogel.³⁹ Equilibrium swelling ratio of the various poly(AAc-AM-SH) superabsorbent hydrogels S₀, S₁, S₃, S₅, S₇, and S₁₀ in the distilled water, 0.01, 0.05, 0.10, 0.50, and 1% saline solutions (NaCl, MgCl₂, FeCl₃) were investigated and are shown in Figures 6–8, respectively. It was observed from the Figures 6–8 that samples incorporated with SH shows higher equilibrium swelling ratio than the PAAc/AM superabsorbent hydrogels. It can be explained with the fact that incorporated SH improved the network structure of PAAc/AM. Sample S₅ shows the highest equilibrium swelling ratio in various saline solutions. It signifies that an appropriate amount of SH improves the salt resistance of PAAc/AM superabsorbent hydrogel. It can also be observed that equilibrium swelling ratio of superabsorbent was appreciably decreased comparing to the values measured in the distilled water and goes on decreasing as the ionic concentration of the salt solutions increases. This is associated with the decrement in expansion of the

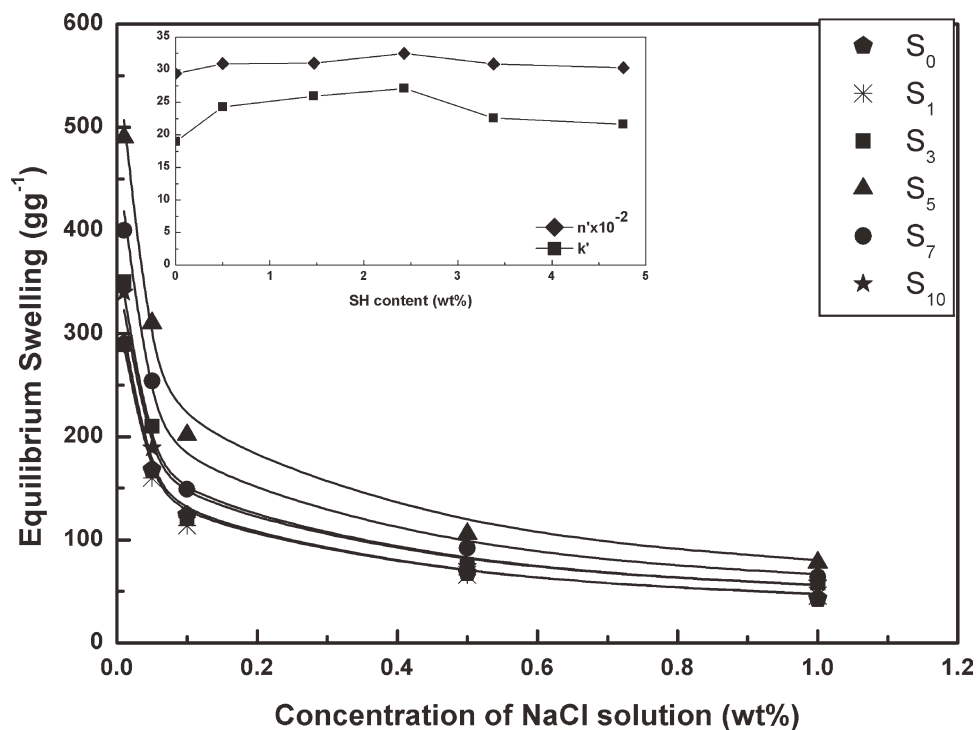


Figure 6 Equilibrium swelling ratios of AAC-AM-SH superabsorbent hydrogels in $\text{NaCl}_{(\text{aq})}$ solutions with different concentrations.

gel network because of repulsive forces of counterions on the polymeric chain shielded by the bound ionic charge, therefore, the osmotic pressure differ-

ence between the gel network and the external solution decreased with increase in the ionic strength of the saline concentration.³⁶ Furthermore, the water

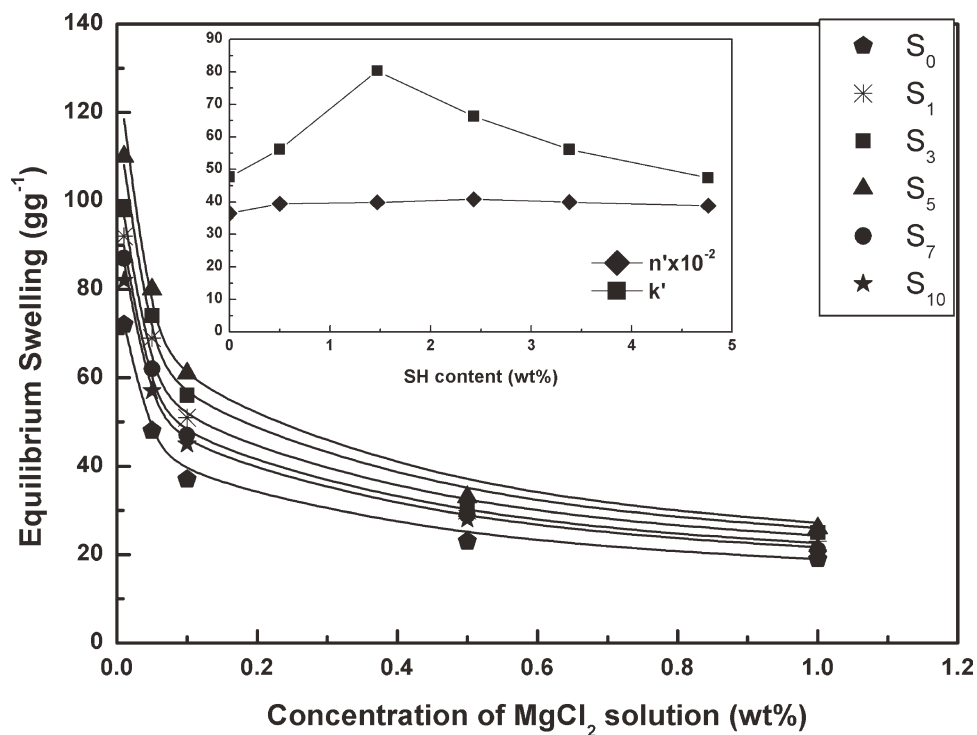


Figure 7 Equilibrium swelling ratios of AAC-AM-SH superabsorbent hydrogels in $\text{MgCl}_{2(\text{aq})}$ solutions with different concentrations.

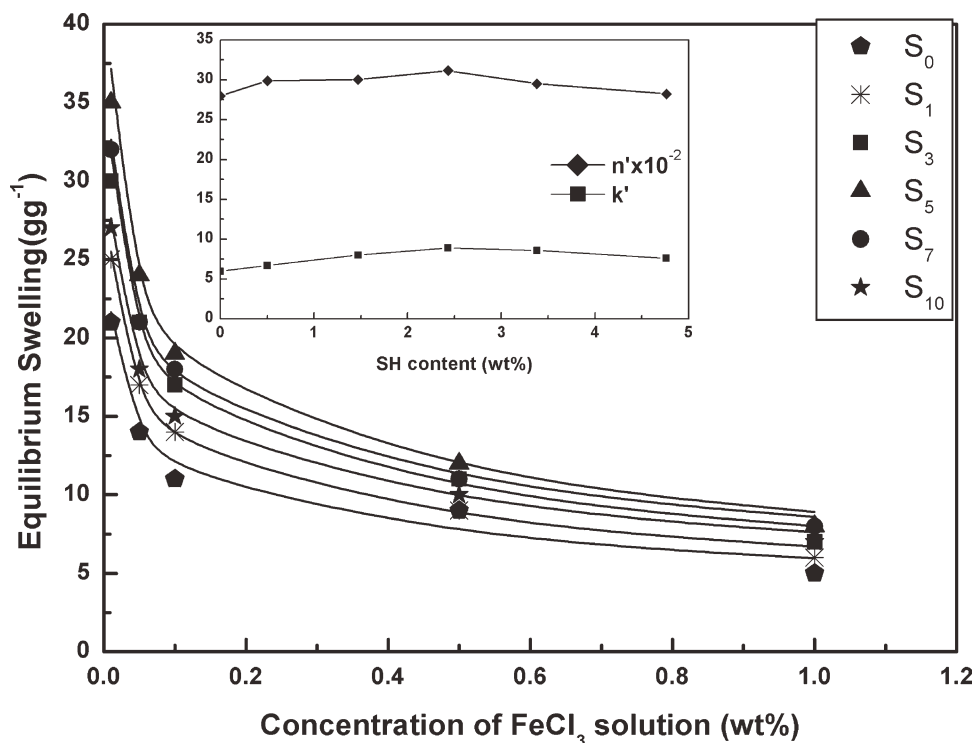


Figure 8 Equilibrium swelling ratios of AAc-AM-SH superabsorbent hydrogels in FeCl_{3(aq)} solutions with different concentrations.

absorbencies for these six superabsorbent hydrogels decreased in the order NaCl > MgCl₂ > FeCl₃. These results are acceptable because with increase in the size of the ions present in the swelling medium decreases the swelling capacity of the superabsorbents due to difficulty in penetration of ions into the networks of polymers. An additional reason is increasing electrostatic attraction between anionic sites of chains and multivalent cations (Mg⁺², Fe⁺³) leading to increased ionic crosslinking degree and consequently loss of swelling. These effects of cations on the equilibrium swelling ratio of superabsorbent are obvious according to many studies.^{40,41}

There is a familiar power-law relationship between swelling and concentration of a salt solution which is stated as following relation,³⁹

$$\text{Equilibrium Swelling} = k'(\text{salt})^{-n'} \quad (11)$$

where k' and n' are power-law constants for an individual superabsorbent that can be obtained from the curve fitted with eq. (11). The calculated constants are listed in the Table III. The k' value is swelling at a high concentration of salt and n' value is a measure of salt sensitivity. Figures 6–8 illustrates the power-law relationship between swelling and saline concentrations. The exponent increases with increasing the SH concentration from 0.50 to 2.43 wt % and then it decreases with a further increase in the SH concentration to 4.76 wt %.

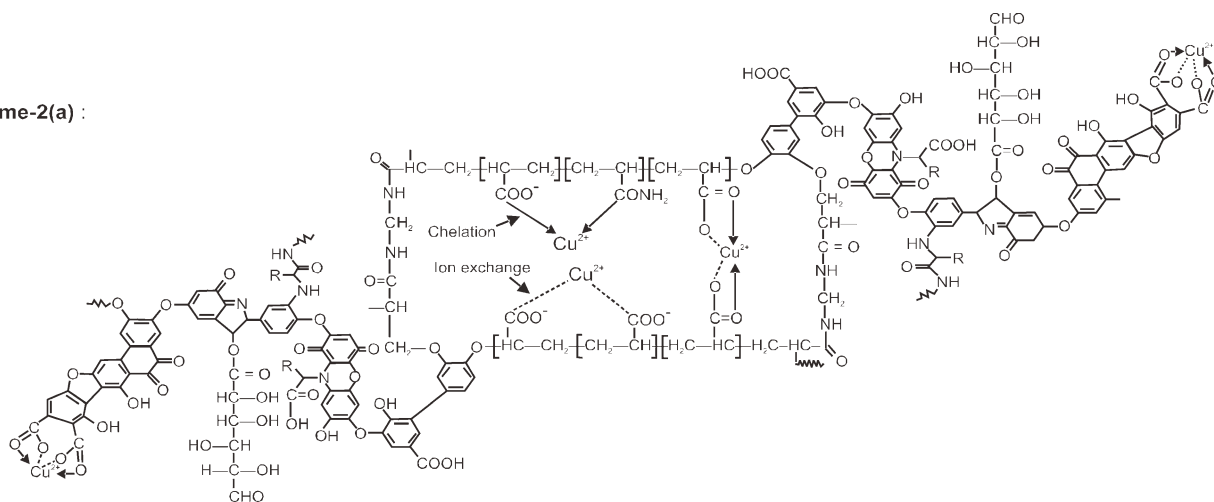
Mechanism of metal ion/dye adsorption

Many studies have been made on the binding of metal ions/dye to polyelectrolytes. Interaction between the metal ions/dye and superabsorbent occur mainly due to electrostatic forces and the formation of coordinate bonds.²¹ These interactions take place at adsorbent/adsorbate interface. In this study, adsorption occurs through the phenolic hydroxyls and carboxylates as the superabsorbent having carboxylic and phenolic groups have high affinities for cationic dyes/metal ions.^{17,42} In the case of Cu²⁺ ions adsorption is mainly because of ion exchange and chelation (Scheme 2a), which may be preceded by long range attractive electrostatic interactions, as the Cu²⁺ ion is condensed on the polymer surface, it is site fixed by the polymer ligands.

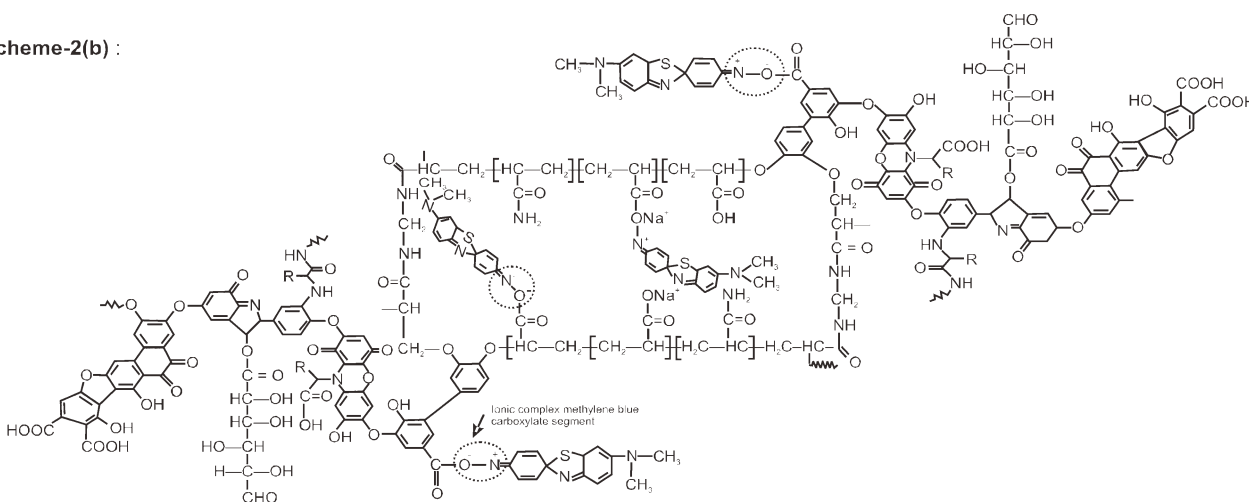
TABLE III
The Power Law Constants [eq. (11)] for Swelling Dependency of Different Samples on Salt Concentration (0.01–1 wt %) of Different Salt Solutions

Sample designation	NaCl		MgCl ₂		FeCl ₃	
	$n' \times 10^2$	k'	$n' \times 10^2$	k'	$n' \times 10^2$	k'
S ₀	36.50	47.42	29.42	18.96	27.98	5.96
S ₁	39.40	47.70	30.92	24.28	29.89	6.70
S ₃	39.88	56.17	31.01	25.95	30.04	8.01
S ₅	40.80	80.36	32.48	27.14	31.18	8.91
S ₇	39.90	66.36	30.87	22.57	29.51	8.58
S ₁₀	38.84	56.11	30.31	21.63	28.24	7.61

Scheme-2(a) :



Scheme-2(b) :



Scheme 2 (a) Mechanism of removal of copper ions by the superabsorbent hydrogel poly(AAc/AM/SH). (b) Mechanism of removal of MB dye molecules by the superabsorbent hydrogel poly(AAc/AM/SH).

For the methylene blue dye, adsorption occur through the formation of an ionic complex between the superabsorbent hydrogel and MB molecules, which formed between imines groups of MB dye and charged functional group of superabsorbent hydrogel (Scheme 2b) as well as because of hydrogen bonding.

Effect of SH content on metal ion/dye adsorption

Figures 9 and 10 shows the effect of SH content on MB dye molecules and Cu^{2+} ions adsorption capacity for PAAc/AM/SH superabsorbent hydrogels S_0 , S_1 , S_3 , S_5 , S_7 , and S_{10} , respectively. It can be examined from Figure 9 that for the MB molecules at the adsorption equilibrium the adsorption capacities are found to be i.e., 241, 218, 252, 269, 220, and 209 mg/g/L for S_0 , S_1 , S_3 , S_5 , S_7 , and S_{10} , respectively. Figure 10 shows the adsorption capacities for Cu^{2+} ions be 239, 249, 274.1,

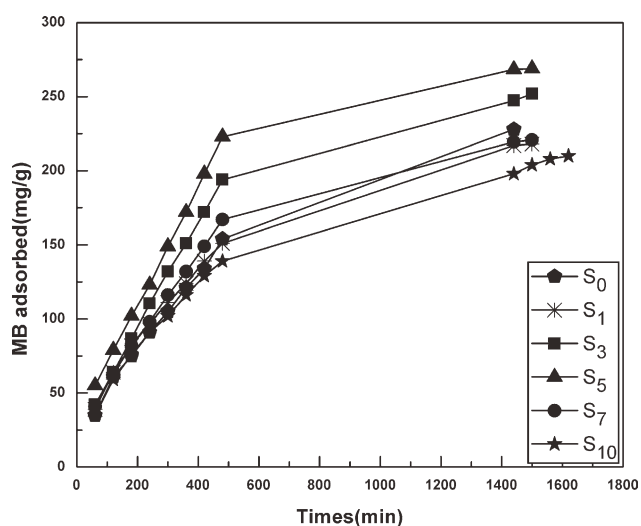


Figure 9 Influence of SH concentration on the adsorption capacity for MB molecules of AAc/AM/SH hydrogels with different amount of SH content.

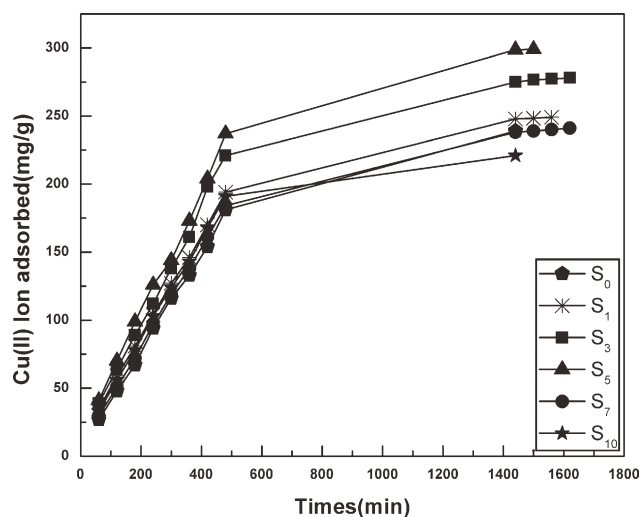


Figure 10 Influence of SH concentration on the adsorption capacity for Cu²⁺ ions of AAC/AM/SH hydrogels with different amount of SH content.

299, 241, and 221 mg/g/L for S₀, S₁, S₃, S₅, S₇, and S₁₀, respectively. The results of sorption and swelling studies are parallel character to each other. The re-

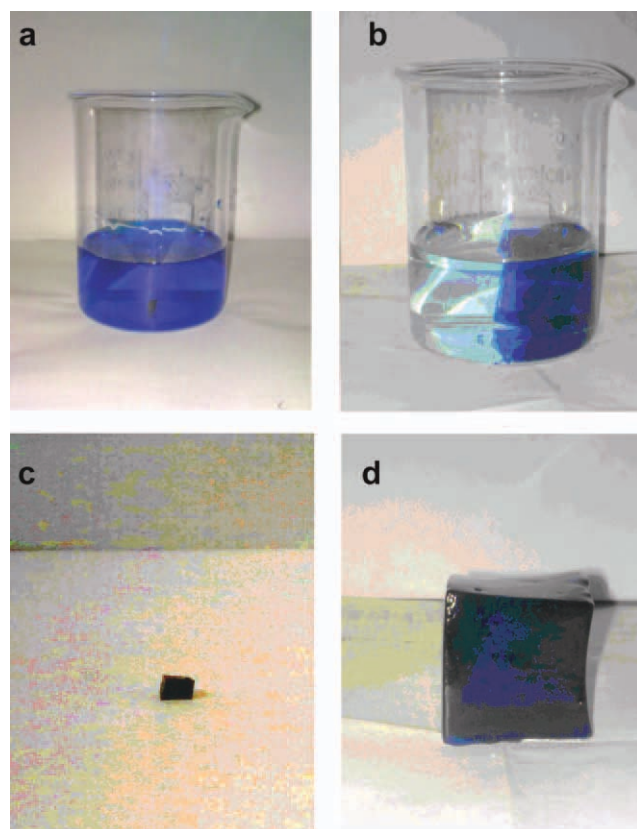


Figure 11 Photographs of MB dye solutions: (a) At the time of immersion and (b) After adsorption (c) S₅ superabsorbent hydrogel before adsorption of dye, and (d) Superabsorbent hydrogel after adsorption of dye. [Color figure can be viewed in the online issue, which is available at wileyonlinelibrary.com.]

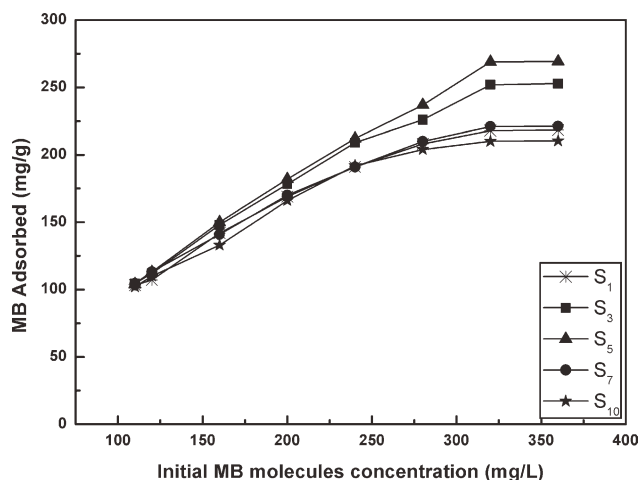


Figure 12 Variation in the adsorption capacity as function of initial MB molecules concentration using superabsorbent hydrogel AAC/AM/SH with the different amount of SH.

moval concentration for Cu²⁺ ion and MB molecules increased initially for S₁–S₅, and then it levels off from S₅ to S₁₀. It indicates that initially there is strong electrostatic attraction between the SH and Cu²⁺ ions/MB molecules and it is assigned to the improved network structure of AAC/AM/SH when compared to AAC/AM. SH can attach to polymer network in the form of grafting by which the network structure improved.⁴³ SH is composed of large number of functional hydrophilic groups that have ability to interact with the Cu²⁺ ions/MB molecules. Also it can be concluded from the above results that an appropriate addition of SH is crucial to improve the adsorption capacity. Similar types of result have been concluded by Yi et al.²⁰ for SH/poly(*N*-isopropylacrylamide) hydrogels that

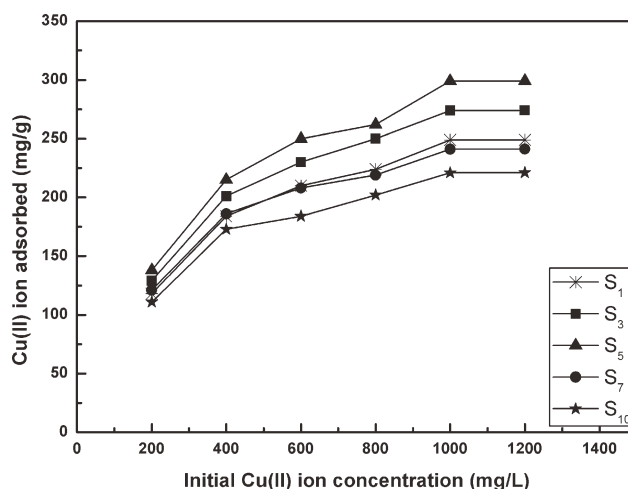


Figure 13 Variation in the adsorption capacity as function of initial Cu²⁺ ions concentration using superabsorbent hydrogel AAC/AM/SH with the different amount of SH.

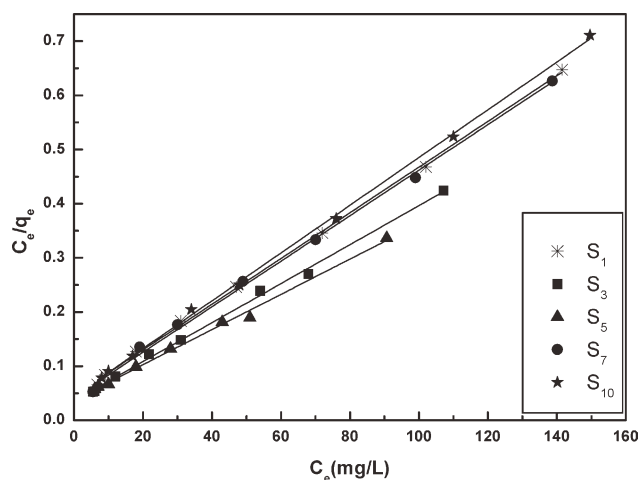


Figure 14 Langmuir adsorption isotherm of MB molecules adsorption on poly(AAc/AM/SH) superabsorbent hydrogels with various SH contents in aqueous solutions.

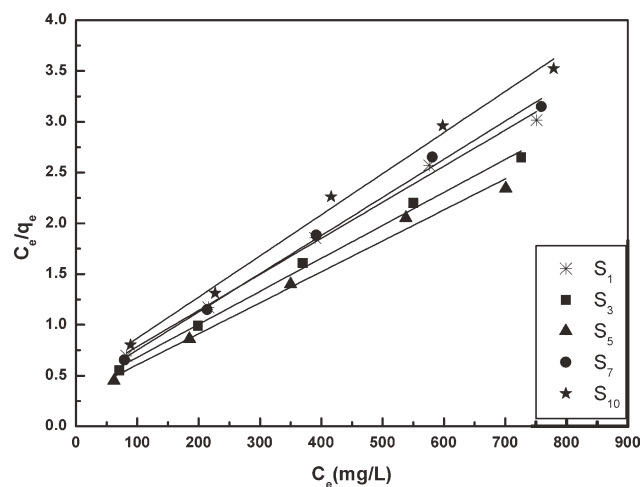


Figure 15 Langmuir adsorption isotherm of Cu^{2+} ions adsorption on poly(AAc/AM/SH) superabsorbent hydrogels with various SH contents in aqueous solutions.

appropriate SH content of hydrogels was crucial for the adsorption and desorption of MB dye. (Fig. 11)

Effect of initial Cu^{2+} ions/MB molecules concentration on adsorption capacity

The dependency of adsorption capacity of the hydrogels S_1 , S_3 , S_5 , S_7 , and S_{10} on the initial concentration of Cu^{2+} ions/MB molecules concentration evaluated by equilibrating the fixed amount of the hydrogel (50 mg) with a series of Cu^{2+} ions/MB dye solutions of gradually increasing concentration. Figure 12 shows dependence of color removal of MB dye molecules as a function of initial concentration of MB dye molecules ranging from 110 to 360 mg/L. Solution with the 320 mg/L shows maximum MB dye removal of 269 mg/g/L for S_5 superabsorbent hydrogel. After that on increasing the concentration to 360 mg/L adsorption capacity decreases to 237 mg/g/L. Adsorption capability of the AAc/AM/SH towards Cu^{2+} ions with different initial Cu^{2+} ions solution concentrations varying from 200 to 1200 mg/L was given in Figure 13. Figure indicates that initially Cu^{2+} ions uptake increased with the increase in ini-

tial concentration of Cu^{2+} ions, and then reached a plateau value. The highest value found to be 299 mg/g/L for S_5 gel obtained from the initial metal ion solution at 1000 mg/L. After increasing a particular value of initial concentration of Cu^{2+} ions/MB molecules; decrement in adsorption binding capacity represents saturation of the active sites (which are available for Cu^{2+} ion/dye). This can be explained, that as the concentration of the MB molecules/ Cu^{2+} ions increases, it results in increase in number of adsorbate, which comes in contact with the adsorbent at the same time interval; whereas the number of sites which are available for adsorption are constant for all concentrations. That is why at higher initial concentration the active site for adsorption becomes fewer.

Adsorption isotherm

Chelation isotherm is used to characterize the interaction of Cu^{2+} ions/MB dye with the superabsorbent hydrogels S_1 , S_3 , S_5 , S_7 , and S_{10} . It provide a relationship between the concentration of Cu^{2+} ions/MB

TABLE IV
Langmuir Coefficients q_{\max} and K_e for the Adsorption of Cu^{2+} Ions and MB Dye on AAc/AM/SH SAHs in Aqueous Solutions Together with the Regression Coefficient (R^2)

Sample designation	Cu^{++} ion				MB dye			
	q_e	q_{\max}	$K_e \times 10^3$	R^2	q_e	q_{\max}	$K_e \times 10^2$	R^2
S_1	249.00	278.00	35.50	0.9949	218	238.00	47.55	0.9985
S_3	274.10	303.03	32.00	0.9961	252	277.77	37.00	0.9939
S_5	299.00	333.33	37.87	0.9904	269	312.50	40.26	0.9837
S_7	241.20	263.16	35.95	0.9956	221	238.10	42.46	0.9948
S_{10}	221.06	243.90	51.26	0.9936	210	227.27	47.00	0.9990

TABLE V
Comparison Table for Removal Capacities (q_e) of Cu^{2+} Ions and MB Dye by Various Adsorbents

Cu ⁺⁺ ion			MB dye		
Absorbent	q_e (mg/g)	Reference	Absorbent	q_e (mg/g)	Reference
Amine functionalized silica	9.02	(46)	Alginate/polyaspartate	4.85	(50)
Chitosan	17.9	(47)	Clay	58.2	(51)
N,O-carboxymethyl- Chitosan	162.5	(48)	SH	48	(52)
Acid-activated polygorskite	32.24	(49)	Sodium humate/Poly (N-isopropylacrylamide)	10.8	(20)
Poly(AAc-AM-SH)	299	This work	Poly(AAc-AM-SH)	269	This work

molecules dye in the solution and the amount of Cu^{2+} ions/MB molecules adsorbed on to the solid phase when two phases are at equilibrium. The data for the uptake of Cu^{2+} ions/MB molecules by superabsorbent hydrogels AAc/AM/SH have been analyzed in light of Langmuir isotherm model of adsorption. The Langmuir adsorption isotherm equation is represented as⁴⁴

$$\frac{C_e}{q_e} = \frac{1}{K_e q_{\max}} + \frac{C_e}{q_{\max}} \quad (12)$$

where C_e is the equilibrium concentration mg/L, q_e the amount adsorbed at equilibrium mg/gm/L, K_e and q_{\max} are Langmuir constants related to energy of adsorption and adsorption capacity i.e., the amount of adsorbate required covering a monolayer. The plots of Langmuir adsorption isotherm of MB molecules and Cu^{2+} ions are shown in Figures 14 and 15, respectively. The plots appear to be linear over the whole concentration range studied. The value of q_{\max} and K_e were calculated from the slope and intercept of linear plots of C_e/q_e vs. C_e and tabulated in Table IV together with regression coefficients. The calculated monolayer adsorption capacity q_{\max} for MB molecules 238.00, 277.77, 312.50, 238.10,

and 227.27 mg/gm/L for $S_1, S_3, S_5, S_7, S_{10}$, respectively and for Cu^{2+} is found to be 278.00, 303.03, 333.33, 263.15, and 243.90 mg/gm/L. The q_{\max} values of the superabsorbent hydrogels obtained by Langmuir equation were quite consistent with the experimental one (Table IV). The applicability of Langmuir model and higher values of regression coefficient (R^2 value found in the range of 0.9897–0.9990 and 0.9904–0.9961 for MB dye molecules and Cu^{2+} ions, respectively) suggest favorable and monolayer adsorption.⁴⁵

When the equilibrium adsorption of Cu^{2+} ion and MB dye of our S_5 hydrogel was compared with the work of other researchers (shown in Table V); it was evident that the synthesized S_5 superabsorbent hydrogel has a very high adsorption capacity of 299 and 269 mg/L for Cu^{2+} ion and MB dye, respectively; indicating that it can be effectively and economically used as wastewater purifier.

Desorption/regeneration of adsorbent

For any adsorption process the recovery and regeneration of adsorbent are important factors. Desorption studies may help to recover the Cu^{2+} ions/MB dye molecules from the adsorbent and regenerate

TABLE VI
Adsorption Amount of Cu^{2+} Ion and MB Dye After Repeated Adsorption–Desorption Cycle

Cycle no.	S_1		S_3		S_5		S_7		S_{10}		
	A	D	A	D	A	D	A	D	A	D	
Cu^{2+} ion	1	249.0	97.5	274.0	97.4	299.0	98.2	241.0	96.5	221.0	96.1
	2	248.4	98.1	273.6	97.2	298.8	98.4	240.7	96.6	220.0	96.5
	3	248.0	98.6	273.1	97.6	298.4	98.1	240.3	96.1	219.7	96.0
	4	247.6	98.2	272.8	96.9	298.2	97.8	239.5	95.9	219.5	97.1
	4	247.6	98.2	272.8	96.9	298.2	97.8	239.5	95.9	219.5	97.1
MB dye	5	247.1	97.9	272.2	96.5	297.7	97.8	239.1	96.2	218.8	97.0
	1	218.0	94.1	252.0	93.4	269.0	95.58	221.0	92.4	210.0	90.2
	2	217.6	94.6	251.8	93.4	268.48	95.10	220.88	92.7	209.5	90.8
	3	217.4	95.1	251.4	93.8	268.10	95.30	220.41	91.5	209.3	90.4
	4	217.1	94.0	250.4	92.9	267.87	94.84	220.11	93.1	208.8	89.3
5	216.7	94.7	250.1	93.7	267.54	95.11	219.74	92.4	208.3	90.4	

A, Adsorption (mg/g); D, Desorption (%).

the superabsorbent hydrogel. Because of which it can be used again and again for the adsorption. Elution of Cu^{2+} ions/MB dye molecules was also studied in a batch experimental set up. The AAc/AM/SH superabsorbent hydrogels which were used for the adsorption of Cu^{2+} ions/MB dye were placed in elution medium for 24 h and the amount of Cu^{2+} ions/MB dye desorbed to the elution medium was measured. As seen in Table VI the polymer showed stable Cu^{2+} ions/MB dye removal capacities after repeated regeneration.

CONCLUSION

Experimental results show that swelling behavior of superabsorbent hydrogel poly(AAc/AM/SH) was significantly dependent on the SH concentrations in a nonlinear fashion. When percentage of SH content increases from 0.50 to 1.47 wt % the swelling ratio shows slight increase from 480 to 523 gg^{-1} and after that it shows drastic increase in swelling ratio. Highest equilibrium swelling ratio of 724 gg^{-1} was obtained for S_5 hydrogel having 2.43 wt % SH concentration. On further increment of SH concentration from 2.43 to 4.76 wt % in the feed, equilibrium swelling ratio decreased from 724 to 389 gg^{-1} . Superabsorbent hydrogels of poly(AAc/AM/SH) exhibited the non-Fickian type diffusion ($0.68 < n > 0.79$) with diffusion coefficients in the range of 35.15×10^{-3} to $51.30 \times 10^{-3} \text{ cm}^2/\text{min}$. The swelling kinetics of the poly(AAc/AM/SH) superabsorbent in water was governed by the Schotts second order equation. Equilibrium swelling ratio of PAAc/AM and PAAc/AM/SH superabsorbent hydrogels in various saline solutions (NaCl , MgCl_2 , and FeCl_3) were investigated; and it can be concluded that SH containing hydrogels always had higher water absorbency as compared to control. The water absorbency of superabsorbent hydrogel for different saline solutions shows the order $\text{NaCl} > \text{MgCl}_2 > \text{FeCl}_3$. The power-law relationships were found for swelling on SH concentration and swelling on saline dependency.

The removal capacity of PAAc/AM/SH superabsorbent hydrogel initially increased with increasing SH concentration and then it goes down. Superabsorbent hydrogel S_5 showed highest removal capacity for both Cu^{2+} ions as well as for MB dye. The maximum binding capacity for Cu^{2+} ion was 299 $\text{mg}/\text{gm}/\text{L}$ at 1000 mg/L initial Cu^{2+} ion concentration and for MB dye it is 269 $\text{mg}/\text{gm}/\text{L}$ at 320 mg/L initial MB dye concentration. Cu^{2+} ion/MB dye adsorption on copolymer superabsorbent hydrogels agrees well with the Langmuir model. On the basis of the earlier results it can be proposed that PAAc/AM/SH superabsorbent hydrogels promise to be potential adsorbents for the removal of heavy metals and dye from waste water and aqueous effluents.

References

- Liu, M. Z.; Liang, R.; Zhan, F. L.; Liu, Z.; Niu, A. Z. *Polym Adv Technol* 2006, 47, 430.
- Clarke, J. B. *Eur Pat.*101,253 (1984).
- Malowaniec, K. D. *U.S. Pat.*6,414,216 B1 (2002).
- Walker, C. O. *U.S. Pat.*4,664,817 (1987).
- Vogt, P.; Roehlen, R.; Tennie, M. E. *P.1,534,515* (2005).
- Hefner, R. E.; Haynes, D. I. *U.S. Pat.*4,611,015 (1986).
- Hosoya, Y.; Watanabe, N.; Takagi, I.; Miyoshi, A. *Eur. Pat.*342,996 (1989).
- Katzer, M. F. *U.S. Pat.*3,354,084 (1967).
- Dong, L. C.; Hoffman, A. S. *J Control Release* 1991, 15, 141.
- Karadag, E.; Saraydin, D.; Oztop, H. N.; Guven, O. *Polym Adv Technol* 1994, 5, 664.
- Karadag, E.; Saraydin, D.; Guven, O. *J Appl Polym Sci* 1996, 6, 2367.
- Oren, S.; Caykara, T.; Kantoglu, O.; Guven, O. *J Appl Polym Sci* 2000, 78, 2219.
- Kara, A.; Uzun, L.; Besirli, N.; Denizli, A. *J Hazard Mater* 2004, B106, 93.
- Demirbas, A. *J Hazard Mater* 2008, 157, 220.
- Beuvais, R. A.; Alexandratos, S. D. *React Funct Polym* 1998, 36, 113.
- Essawy, H. A.; Ibrahim, H. S. *React Funct Polym* 2004, 61, 421.
- Karadag, E.; Saraydin, D.; Guven, O. *Sep Sci Technol* 1995, 30, 3747.
- Rosiak, J.; Burczak, K.; Czolzynska T.; Pekala, W. *Radiat Phys Chem* 1983, 22, 907.
- Wang, W.; Wang, A. *J Appl Polym Sci* 2009, 112, 2102.
- Yi, J. Z.; Ma, Y. Q.; Zhang, L. M. *Bioresource Technol* 2007, 11, 020.
- Li, W.; Zhao, H.; Teasdale, P. R.; John, R. *React Funct Polym* 2002, 43, 4803.
- Liu, J.; Wang, Q.; Wang, A. *Carbohydr Polym* 2007, 70, 166.
- Hua, S.; Wang, A. *Carbohydr Polym* 2009, 75, 79.
- Peniche, C.; Cohen, M. E.; Vazquez, B.; Roman, J. S. *Polymer* 1997, 38, 5977.
- Vazquez, H.; Rodriguez, J. V.; Cruz Ramos, C. *J Appl Polym Sci* 1993, 50, 777.
- Berens, A. R.; Hopfenberg, H. B. *Polymer* 1978, 19, 489.
- Ali, A. E.; Shawky, H. A.; Abd El Rehim, H. A.; Hegazy, E. A. *Eur Polym J* 2003, 39, 2337.
- Karadag, E.; Saraydin, D.; Guven, O. *Nucl Instr Meth B* 2004, 225, 489.
- Yi, J. Z.; Zhang, L. M. *Eur Polym J* 2007, 43, 3215.
- Buchholz, F. L. In *Modern Superabsorbent Polymer Technology*; Buchholz, F. L.; Graham, A. T., Eds.; Wiley: New York, 1997; pp 4-6.
- Dicicco, M.; Duong, T.; Chu, A.; Jansen, S. A. *J Biomed Mater Res* 2003, 65, 137.
- Paciolla, M. D.; Kalla, S.; Jansen, S. A. *Adv Environ Res* 2002, 7, 169.
- Wang, W.; Wang, A. *Carbohydr Polym* 2010, 1, 020.
- Buchanan, K. J.; Hird, B.; Letcher, T. M. *Polym Bull* 1986, 15, 325.
- Lee, W. F.; Wu, R. J. *J Appl Polym Sci* 1996, 62, 1099.
- Peppas, N. A.; Franson, N. M. *J Polym Sci* 1983, 21, 983.
- Solpan, D.; Duram, S.; Guven, O. *J Appl Polym Sci* 2002, 86, 3570.
- Karadag, E.; Saraydin, D.; Caldiran, Y.; Guven, O. *Polym Adv Technol* 2000, 11, 59.
- Murthy, P. S. K.; Mohan, Y. M.; Sreeramulu, J.; Raju, K. M. *React Funct Polym* 2006, 66, 1482.
- Castal, D.; Ricard, A.; Audebert, R. *J Appl Polym Sci* 1990, 39, 11.
- Lee, W. F.; Yeh, P. L. *J Appl Polym Sci* 1997, 64, 2371.
- Saraydin, D.; Karadag, E.; Guven, O. *Sep Sci Technol* 1995, 30, 3287.

43. Hua, S.; Wang, A. *Polym Adv Technol* 2008, 99, 2182.
44. Langmuir, I. *J Am Chem Soc* 1946, 38, 2221.
45. Singh, K. K.; Singh, A. K.; Hasan, S. H. *Biores Technol* 2006, 977, 994.
46. Lin, Y.; Chen, H.; Lin, K.; Chen, B.; Chiou, C. *J Environ Sci* 2011, 23, 44.
47. Ilauro, S. L.; Claudio, A. *Thermochim Acta* 2004, 421, 133.
48. Sun, S. L.; Wang, A. Q. *J Hazard Mater* 2006, 131, 103.
49. Chen, H.; Zhao, Y. G.; Wang, A. *J Hazard Mater* 2007, 149, 346.
50. Jeon, Y. S.; Lei, J.; Kim, J. H. *J Ind Eng Chem* 2008, 14, 726.
51. Gurses, A.; Dogar, C.; Yacin, M.; Acikyildiz, M.; Bayrak, R.; Karaca, S. *J Hazard Mater* 2006, 131, 217.
52. Paulino, A. T.; Guilherme, M. R.; Reis, A. V.; Campese, G. M.; Muniz, E. C.; Nozaki, J. *J Colloid Interface Sci* 2006, 301, 55.